Abstract

Human embryonic stem cells can be differentiated *in vitro* into a wide variety of progeny cells by addition of different morphogens and growth factors. Our aim was to monitor the expression pattern of tight junction (TJ) components and various cellular markers during differentiation of stem cell lines toward the hepatic lineage.

Human embryonic stem cell lines (HUES1, HUES9) were differentiated into endoderm-like cells, and further differentiated to hepatocyte-like cells. Gene expressions of Oct3/4, Nanog, alpha-fetoprotein, albumin, cytokeratins (CK-7, CK-8, CK-18, CK-19), ATP-binding cassette (ABC) transporters (ABCC2, ABCC7, ABCG2), and various TJ components, including claudin-1, claudin-4, claudin-5, claudin-7, and tricellulin, as well as an extracellular matrix component, agrin were monitored during hepatic differentiation by real-time quantitative PCR.

The differentiated cells exhibit epithelial morphology and functional assessments similar to that of hepatocytes. The expression level of stem cell marker genes (Oct3/4 and Nanog) significantly and gradually decreased, while liver-associated genes (alpha-fetoprotein, albumin) reached their highest expression at the end of the differentiation. The endoderm-like cells expressed claudin-1, which declined eventually. The expression levels of cholangiocyte markers including claudin-4, CK-7, CK-19, and agrin gradually increased and reached their highest level at the final stage of differentiation. In contrast, these cells did not express notable level of claudin-7, CK-8 and tricellulin.

The marker set used for monitoring differentiation revealed both hepatocyte and cholangiocyte characteristics of the differentiated cells at the final stage. This is the first report describing the expression level changes of various TJ components, and underlining their importance in hepatic differentiation.

1. Introduction

Human embryonic stem cells provide new possibilities for the clinical treatment of a number of diseases such as diabetes mellitus type 1 [1], Parkinson's disease [2], Huntington's disease [3], cardiac failure [4], etc. In addition, the ability of pluripotent human embryonic stem cells to differentiate into various cell types enables us to utilize them for studying early human development and provides a cell source for cellular model systems.

Human embryonic stem cell-derived cell lines (HUES) [5] can be differentiated toward the hepatic lineage, allowing us to study hepatic differentiation in culture. *In vitro* modeling of the molecular mechanisms of hepatic differentiation could help us better understanding not only normal development, but the pathogenesis of different types of liver cancers. This *in vitro* system could also help to develop therapeutic strategies for primary liver tumors. Of note is that extending the number of functional hepatocytes in a diseased liver would have obvious therapeutic potential [6].

Parenchymal cells of the liver, i.e., hepatocytes and bile duct cells (cholangiocytes) play distinct roles in diverse hepatic functions, thus, they differ from each other in several aspects including expression pattern of cytokeratins, ABC transporter proteins, and tight junction (TJ) components [7-9].

Human adult hepatocytes express cytokeratin-8 (CK-8) and CK-18, whereas intrahepatic bile duct cells also express CK-7 and CK-19 [10, 11]. Consequently, the biliary type cytokeratins, CK-7, CK-8, CK-18, and CK-19 are highly expressed in cholangiocarcinomas [12, 13].

Hepatic ABC transporters greatly contribute to various functions of liver cells. ABCC2 (MRP2) and ABCG2 proteins, residing in the canalicular (apical) membrane of hepatocytes, are responsible for excretion of endo- and xenobiotics into the bile [14, 15]. In contrast, hepatic ABCC7 (CFTR) regulates the movement of chloride and sodium ions across the membrane of bile duct cells [16]. ABCG2 has also been shown to play protective roles in blocking absorption at the apical membranes of hematopoietic progenitor and other stem cells [17]. High levels of ABCG2 expression were reported not only in hepatocytes but also in human embryonic stem cell lines (HUES1 and HUES9) [18, 19]. A recent study suggested new roles for ABCG2 in the regulation of cellular differentiation [20].

TJs, the most apically located junctional complexes, are critical for epithelial cell barrier and polarity functions, and are composed of several proteins [21-24]. Claudins, with 27 subtypes in human cells, together with occludin are the main protein components of bicellular TJs [24, 25]. Tricellulin is a more recently identified protein, which is concentrated mainly at the convergence of three adjacent cells, however, also expressed to a lesser degree in bicellular TJs [26].

In the liver, claudin-1 can be detected in both hepatocytes and cholangiocytes [27, 28], however, claudin-4 can be mainly found in cholangiocytes and tumors of cholangiocyte origin [7, 29]. Claudin-5 component is typically expressed in the endothelial cells [22], however it can be expressed in certain tumors such as in fibrolamellar carcinoma of the liver [27]. In normal liver the hepatocytes were found to be negative for claudin-7 and the normal biliary epithelial cells showed intense basolateral membrane claudin-7 positivity [8, 24, 30].

Cells and tissues are characterized by a highly specific TJ protein composition [31], which might be altered in severeal diseases, especially during carcinogenesis

[23, 32]. Agrin mediate cell adhesion and control the activities of numerous growth and motility factors and play a critical role in carcinogenesis and tumor progression [33, 34].

During cancer development, the expression of several TJ components usually decreases [27, 28, 35], however, elevated expression of TJ components have been detected in certain tumors [9, 36-38]. In contrast to hepatocellular carcinoma (HCC) [7, 39], overexpression of claudin-4 has been observed in cholangiocarcinoma [29], in colon cancer [40], in pancreatic ductal carcinoma [41] and in several other malignancies [37, 42, 43]. Claudin-7 is a prognostic factor for HCC [30]. Survival analysis showed a trend toward a better prognosis among patients with overexpression of claudin-7 in tumor tissues [39]. These data suggest that the overexpression of claudins in certain tumors are useful in diagnostics [29, 36, 40, 41, 44], and may even serve as future therapeutic targets [23, 45].

These data raise the question, whether changes in the expression pattern of TJ components can be detected during hepatic differentiation. Thus, we aimed to characterize the expression pattern of TJ components, mainly claudins, in endoderm-like and hepatocyte-like cells differentiated from HUES cell lines. The differentiated cells were characterized by morphological analysis [46], functional assays, and expression profiles of cytokeratins and ABC transporters characteristic of liver cells.

2. Materials and methods

2.1. HUES cell lines and their culturing

The human embryonic stem cell lines, HUES1 and HUES9, having normal karyotype, were gifts from Dr. Douglas Melton (Harvard University), and were maintained according to the recommended culturing protocol. Briefly, cells were cultured on mitomycin-C treated mouse embryonic fibroblast (MEF) feeder cells in complete HUES medium consisting of 15% knockout serum replacement (Gibco-Invitrogen, Grand Island, NY, USA), 80% knockout Dulbecco modified Eagle medium (KO-DMEM, Invitrogen, Carlsbad, CA, USA), 1 mM L-glutamine, 0.1 mM beta-mercaptoethanol, 1% nonessential amino acids and 4 ng/mL human fibroblast growth factor [18]. For passage, cells were dissociated with the use of a collagenase IV solution (200 U/ml) (Gibco-Invitrogen). The cell culture was conducted in a 5% CO_2 air mixture at 37°C. The medium was changed daily (2ml/well). Karyotype analysis indicated normal karyotype in all experiments [47].

2.2. Hepatic differentiation of HUES cells

HUES cells at 80% confluence in 6-well plates were treated with collagenase IV, transferred to Matrigel-coated (Becton Dickinson, Franklin Lakes, NJ, USA) six-well plates ($3\times10^5/cm^2$), and cultured in MEF-conditioned medium containing 80% KO-DMEM, 2 mM Gluta MAX, 0.1 mM beta-mercaptoethanol, 4 ng/ml basic fibroblast growth factor (bFGF) (R&D Systems, Minneapolis, MN, USA) for 3 days, while maintaining undifferentiated status. For coating, prior to seeding, the six-well plates were incubated with Matrigel diluted 1:20 in cold KO-DMEM at 4°C at least overnight [48]. To produce MEF-conditioned medium, Mitomycin-C treated mouse

embryonic fibroblast feeder cells were seeded at 55 000 cells/cm^2 density in MEF medium consisting of DMEM containing 4.5 g/L glucose and 10% fetal bovine serum (FBS) (Gibco-Invitrogen). After at least 4 h, the medium was replaced with HUES medium (mentioned above) (0.5 ml/cm^2). Conditioned media was collected daily for 7-10 days.

For endodermal differentiation, cells were cultured in DMEM/F-12 medium (Gibco-Invitrogen) supplemented with 1% fetal bovine serum (FBS) (Gibco-Invitrogen), 1% BSA (Sigma, St. Louis, MO, USA), 100 U/ml penicillin and streptomycin (Sigma), 2 nM glutamine, and 50 ng/ml human activin A (R&D Systems) [49] for 5 days.

For hepatic differentiation, HUES1 and HUES9 cells were cultured in DMEM/F-12 medium supplemented with 10% FBS, 1% BSA, 100 U/ml penicillin and streptomycin (Sigma), 2 nM glutamine, and 20 ng/ml hepatocyte growth factor (HGF, R&D Systems) [49, 50] without activin A for 7 days.

Throughout the entire 15-day differentiation protocol, the medium was changed every other day, and the cells were collected at well characterized stages of the differentiation process; at day 0 HUES cells, at day 3 undifferentiated cells, at day 8 endoderm-like cells and at day 15 hepatocyte-like cells.

2.3. Morphological and functional characterization of differentiated cells.

During the time of culture, morphological changes (shape, granularity) were analyzed by phase contrast microscopy (Olympus CKX41, Olympus, Tokyo, Japan).

Glycogen storage was determined by Periodic Acid-Schiff (PAS) assay (Sigma). Cells attached to the dish were washed with PBS three times and fixed with PBS supplemented with 4% paraformaldehyde (Wako Pure Chemical Industries,

Osaka, Japan) at room temperature for 30 min. Cells were then oxidized with 1% periodic acid (Sigma) for 10 min, washed with distilled water three times, incubated with PAS reagent (Sigma) for 15 min and rinsed with distilled water for 10 min [51, 52]. The PAS staining was examined with an Olympus CKX41 inverted, fluorescence microscope.

The indocyanine green (ICG) (Sigma) uptake test of the differentiated cells [51, 52] was performed as follows: The ICG solution (1mg/ml in medium) was added to the cell culture dish and incubated at 37°C for 15 minutes. After rinsing the dish three times with PBS, the cellular uptake of ICG was examined with an Olympus CKX41 inverted, fluorescence microscope. Following examination, the dish was refilled with DMEM containing 10% FBS. Loss (release) of cellular ICG stain was examined 6 hours later.

2.4. Quantitative PCR analyses

Total RNA was isolated from 5-10×10^6 cells using TRIzol Reagent (Invitrogen). RNA transcripts were purified by phenol/chloroform extraction and ethanol precipitation [53]. Absorption levels of RNA extracts were obtained using NanoDrop Spectrophotometer ND-1000 (Promega, San Luis Obispo, CA, USA). cDNA samples were prepared from 1 μg total RNA using Promega Reverse Transcription System Kit (Promega). The RT-PCR primers were designed to flank a region that contained at least one intron. The data of applied primer sequences are listed in *Table 1*. Several housekeeping genes were tested in the current study (GAPDH, cyclophilin, 36b4, 18S ribosomal RNA, beta-2-microglobulin, TATA box binding protein, ABL). ABL (Abelson tyrosine-protein kinase 1) was found to be the

best control gene for quantitative RT- PCR in the hepatic differentiation model system.

RT-PCR analysis was performed using SYBR Green technology on a Light Cycler 480 real-time PCR system (Roche Diagnostics, Burgess Hill, West Sussex, UK) according to the manufacturer's instructions. The final 10 µl reaction mixture contained 5 µl LightCycler FastStart DNA Master SYBR Green I (Roche Diagnostics), 1 µl of 2.5 µM forward and reverse primers, 2 µl of water, and 1 µl of template cDNA. Cycling was performed using the following amplification conditions: One cycle at 95°C for 5 min was followed by 45 cycles at 95°C for 30 s, 61°C for 10 s and 72°C for 10 s with subsequent heating to 95°C for 20 s, cooling to 45°C for 10 s and reheating to 95°C at a rate of 0.11°C/s. Primer specific amplification was checked by 2% (w/v) agarose gel electrophoresis as well as melting temperature (Tm) analysis.

The delta-delta cycle threshold (CT) method was used for the gene expression assays. Statistical analysis was performed using STATISTICA 8 software (StatSoft, Tulsa, OK, USA). “Nonparametric method” and “comparing multiple independent samples” was used to assess differences between the well characterized stages of the differentiation. Kruskal-Wallis ANOVA and Median Test ‘p’ values less than 0.05 were considered as statistically significant. Data are representative from three independent experiments.

2.5. Immunostaining of differentiated cells

For immunofluorescence staining of TJ components, HUES9 cells were seeded onto Imaging dishes (no. 5160, Zellkontakt, Nörten-Hardenberg, Germany), and differentiated as detailed in Section 2.2. The differentiated cells at the final stage

were fixed and permeabilized with ice cold methanol for 15 minutes, and labeled with primary antibodies against claudin-1 (1:100), claudin-4 (1:100), claudin-5 (1:120), claudin-7 (1:100), and tricellulin (1:50) antibodies for 2 hours, following a one hour blocking with Dulbecco's modified PBS containing 2 mg/ml BSA, 1% fish gelatin, 0.1% Triton X-100, and 5% goat serum (pH 7.2). AlexaFluor-488-conjugated anti-mouse and anti-rabbit IgG secondary antibodies were used (1:250). The antibodies were obtained from Life Technologies/Thermo Fisher Scientific (Waltham, MA, USA) with the exception of anti-claudin-1 antibody, which was from Cell Marque (Rocklin, CA, USA). The cell nuclei were stained with 1 μM DAPI in DPBS for 10 minutes. The blue and green red fluorescence of stained samples was studied by an Olympus FV500-IX confocal laser scanning microscope using a PLAPO 60× (1.4) oil immersion objective (Olympus) at 405 and 488 nm excitations, respectively.

3. Results

3.1. Morphological and functional characterization of HUES cell-derived hepatocyte-like cells

A three-stage hepatic differentiation protocol depicted in *Figure 1a* was performed with two human embryonic cell lines, HUES1 and HUES9. To evaluate the progression of differentiation, the cells were characterized at four critical points of differentiation. These phases are the original HUES9 cell line, the embryonic stem cells on Matrigel after 3 days (undifferentiated stage), the cells following a 5-day activin A treatment (endodermal stage), and the hepatocyte-like cells at the end of the differentiation (hepatic stage). First, the morphological parameters of the cells were analyzed by microscopy at the end of each stage *(Figure 1b-e).* By the end of differentiation HUES9 cells developed into cells, which exhibited polygonal shape and were enriched in cytoplasmic granules, which morphology is characteristic of human hepatocytes in culture.

Next, glycogen storage of the differentiated cells was assayed by Periodic Acid-Schiff (PAS) staining to confirm this characteristic feature of hepatocyte functions. The hepatocyte-like cells derived from HUES9 cells generated and accumulated substantial amount of glycogen *(Figure 2b).* PAS positivity of differentiated cells was paralleled with the hepatocyte-like morphology. No glycogen accumulation was observed in adjacent cell populations showing fibroblast-like morphology, or in undifferentiated HUES9 cells *(Figure 2a)*. As positive control for PAS staining, primary cultures of rat hepatocytes were used *(Figure 2d)*, whereas MDCK (Madin-Darby canine kidney) cells served as negative control for these experiments *(Figure 2c).*

As another assessment of hepatocyte functions, uptake and release of indocyanine green (ICG) dye were measured in hepatocyte-like cells differentiated from HUES9 cells. Differentiated cells accumulated ICG from the medium and subsequently released the absorbed dye *(Figure 2e, f),* demonstrating the functionality of hepatic transport processes in the HUES9-derived hepatocyte-like cells. In contrast, no ICG accumulation was observed in undifferentiated HUES9 confirming the specificity of the assay *(Figure 2g, h)*.

Both morphological and functional assessments demonstrated typical hepatic characteristics of the cells differentiated from HUES9 cells. In contrast, the cells originated from the HUES1 cell line did not exhibit hepatic features, as neither glycogen production nor ICG accumulation was observed in these cells (data not shown).

3.2. The expression levels of stage-specific differentiation marker genes

To monitor the progression of hepatic differentiation of HUES9 cells, the mRNA expression levels of a series of differentiation marker genes were determined by quantitative RT-PCR at the four characteristic stages of differentiation. To make quantitation of PCR more reliable, the expression levels of a numerous housekeeping genes including GAPDH, cyclophilin, 36b4, 18S ribosomal RNA, beta-2-microglobulin, TATA box binding protein, and ABL were determined at each differentiation stage (not shown). Out of the studied housekeeping genes, ABL was found to be the most stable gene during hepatic differentiation, thus, ABL was used as a reference gene in the subsequent experiments.

As demonstrated in *Figure 3a*, expression levels of pluripotency markers, such as Oct 3/4 and Nanog rapidly declined during hepatic differentiation of HUES9

cells (50-fold and 40-fold), whereas liver-specific genes, such as alpha-fetoprotein (AFP) and albumin (ALB) were remarkably induced (2500-fold and 500-fold, respectively). The mRNA expression levels of cytokeratins, including CK-7, CK-8, CK-18, and CK-19 were also monitored during HUES9 cell differentiation *(Figure 3b),* and found that CK-7 expression was significantly increased by the end of the differentiation (120-fold), whereas CK-19 showed only a slight and gradual raise. In contrast, expression of CK-8 and CK-18 was not significantly altered during hepatic differentiation of HUES9 cells *(Figure 3b).*

Taken together, the expression pattern of stage-specific differentiation marker genes demonstrate that HUES9 cells can be differentiated into hepatocyte-like cells. It is noteworthy that cells differentiated from HUES1 cells did non exhibit hepatic character in terms of expression of liver-specific markers (data not shown). Given that HUES1-derived differentiated cells lack of hepatic functions and marker genes, in subsequent experiments we focused only on hepatocyte-like cells differentiated form HUES9 cells.

3.3. The gene expression levels of hepatic ABC transporter genes

Since numerous ABC transporter proteins play essential role in various hepatic functions, the expression levels of selected ABC transporters, such as ABCG2, ABCC2, and ABCC7 were determined during the course of hepatic differentiation of HUES9 cells. In accordance with previous reports [18-20], we observed substantial mRNA level of ABCG2 in the parental HUES9 cells, which expression rapidly declined, when the cells were seeded onto Matrigel, and further decreased during endodermal induction *(Figure 4).* However, hepatic maturation of the cells resulted in significant induction in the ABCG2 expression (20-fold)

surpassing the level found in the original HUES9 cell line. The expression of the hepatocyte-specific ABC transporter, ABCC2 significantly increased during hepatic differentiation of HUES9 cells (30-fold). Surprisingly, ABCC7 expression was also significantly induced in the HUES9 cell-derived differentiated bile duct cells (80-fold) *(Figure 4).*

3.4. The gene expression levels of the hepatic tight junction genes

Gene expressions of TJ components were also monitored at various stages of differentiation. As demonstrated in *Figure 5*, gene expression levels of claudin-1 and claudin-4 were induced significantly (30-fold and 20-fold) during hepatic differentiation of HUES9 cells. In normal liver, claudin-1 is expressed in both hepatocytes and cholangiocytes. In our experiment the endoderm-like cells expressed higher levels of claudin-1, which declined by the end of the differentiation. The gene expression of the cholangiocyte-specific claudin-4 gradually increased and was the highest at the end of the differentiation. Claudin-5 expression only modestly increased during the hepatic differentiation. The gene expression of the biliary epithelial cell-specific claudin-7 showed no significant changes during differentiation *(Figure 5).*

The extracellular matrix component, agrin, which mediate cell adhesion, was induced significantly during hepatic differentiation (10-fold) *(Figure 5).* However, the gene expression of tricellulin was not changed significantly *(Figure 5).* The difference seen in gene expression levels of agrin and tricellulin indicates that the formation of cell junctions is still in an initial phase.

Taken together, the expression pattern of the hepatic tight junction genes suggests the presence of both hepatocyte-like and cholangiocyte-like cells in the culture differentiated from HUES9 cells.

3.5. Expression and subcellular localization of tight junction proteins

To study the protein expression of TJ components in the HUES9-derived differentiated cells, immunofluorescence staining and confocal imaging were performed with the cell cultures at the final stage *(Figure 6)*. The presence of claudin-1, -4, -5, -7, and tricellulin proteins in the HUES9-derived hepatic cells was verified by these experiments. Claudin-1, -5, and tricellulin were clearly localized to the cell periphery, whereas claudin-4 and -7 exhibited also some intracellular (mostly submembrane) staining in addition to the predominant membrane localization. In contrast to the other studied TJ components, claudin-1 was not uniformly localized to the plasma membrane, but exhibited patchy distribution at the periphery of the HUES9-derived hepatocyte-like cells.

4. Discussion

It has been proposed that most epithelial tumors originate from cancer stem cells (CSCs) or tumor initiating cells (TICs) with stem cell-like properties, including self-renewal and multilineage differentiation capacity [42, 54]. Stem cell lines can be differentiated to hepatocyte-like cells implementing an *in vitro* model for the cancer cell formation from tissue stem cells [55]. During the differentiation process the continuous changes in the expression level of various genes can also be monitored [18, 23, 56-58].

The liver is a good objective for studying tissue stem cell differentiation into tumor tissue cells *in vitro* [55], since several stem cells lines can differentiate and regenerate into functional liver cells [59] , and effective hepatic differentiation protocols have already been established [49-53, 60]. It has also been demonstrated that the *in vitro* produced hepatocyte-like cells transplanted into patients can differentiate into functional liver cells [6]. Human embryonic stem cells are pluripotent cells derived from the inner cell mass of blastocyst stage embryos [47, 61]. Pluripotent embryonic stem cells can be differentiated into cells of all three germ layers by adding different morphogens and growth factors [5]. A number of human embryonic stem cell lines are available by now, with well documented characteristics [47, 57]. For the current study, HUES1 and HUES9 as human embryonic stem cell lines were used. There are a number of models, based on which human embryonic stem cell lines are differentiated into hepatic direction [51, 53, 60]. The differentiation protocol applied in our study is straight forward and characterized with well-defined differentiation stages [49, 50].

By way of various methods – morphology studies, PAS staining, ICG uptake and release measurement, mRNA expression profiling of stem cell and hepatocyte marker genes – we demonstrated the capability of HUES9 cells to differentiate to the hepatic lineage. In contrast, the cells differentiated from HUES1 cells didn't show hepatic characteristics. Although a pluripotent stem cell by definition is expected to be able to differentiate toward any somatic lineages, the human stem cell lines originated from the inner cell mass of embryos are not in ground state pluripotency [62]. Since the different HUES cell lines are originated from distinct embryos, and their establishment procedures were also diverse, an intrinsic differentiation bias of the various HUES stem cell lines can be observed. The favored differentiation directions of the 17 different HUES stem cell lines have been previously documented in a detailed report [63].

A set of marker genes specifically expressed in the liver allows us to follow the progress of hepatic differentiation [51, 60], whereas the stem cell character can be monitored by pluripotency marker genes [57]. In the current study, the gene expression of Oct3/4 and Nanog significantly decreased during the hepatic differentiation of HUES9 cells, and these genes were not expressed by the end of differentiation, suggesting that HUES9 cells gradually lost their stem cell characteristics during the differentiation process. AFP is a marker of endodermal differentiation and early fetal hepatocytes [51, 60]. ALB is the most abundant protein synthesized by functional hepatocytes [52]. The gene expression patterns of AFP and ALB imply that the cells differentiated from HUES9 stem cells exhibit immature hepatocyte characteristics.

Cytokeratins (CK) constitute the cytoskeleton of intermediate filament type in most epithelial cells [51] and are abundantly expressed in polarized hepatocytes [10,

11, 13, 59]. The gene expression of ductal marker CK-7 was significantly increased in HUES9 cell-derived differentiated cells, and the gene expression of CK-19, which is normally expressed in biliary epithelial cells and hepatoblasts, was gradually increased in the course of our differentiation experiments. RT-PCR analyses of the hepatic marker genes and CKs suggested the presence of immature hepatocytes and cholangiocytes.

With regard to the hepatic ABC transporters, the gene expression of ABCC2 (MRP2), which is normally expressed in the canalicular (apical) membrane of polarized hepatocyte cells [15], was significantly induced in our experiments, indicating that the differentiated cells are almost fully polarized, functional hepatocytes. ABCC7 (CFTR) is expressed in the epithelia by intrahepatic and extrahepatic bile duct cells in the apical domain [16, 64]. ABCC7 significant gene expression pattern suggest the presence of cholangiocytes and immature hepatocytes as it has been demonstrated in our study. The transient decline and significant regain of ABCG2 expression during hepatic differentiation of HUES9 cells is consistent with the literature data reporting high expression of ABCG2 in both stem cells and hepatocytes [18, 20, 58]. In summary, mRNA expression profiles of the studied ABC transporters suggest that the differentiated cells are similar to mature hepatocyte, and possess transient, bipotential characteristics.

TJs play important role in hepatic differentiation, regeneration, and hepatocarcinogenesis [56, 65]. To date the cell contacts and different components of TJs have not been studied during human embryonic stem cell differentiation into hepatic direction. In the current work, we demonstrated the expression of various TJ components including claudin-1,-4, -5, -7 and tricellulin in the HUES-9-derived hepatic cells at both mRNA and protein levels. The changes in their expression levels

and that of an extracellular matrix protein, agrin at different stages of the hepatic differentiation were also demonstrated.

Claudins are the main transmembrane proteins of TJs. By separating the sinusoidal (basolateral) and bile canalicular (apical) plasma membrane domains, claudins have an important barrier function and are responsible for the polarization of hepatocytes [24, 25, 27, 64]. These TJ components are associated with both cell polarity and permeability [24, 25, 43]. The combination and mixing ratios of claudin isoforms determine the paracellular permeability in TJs [31, 32]. Claudins have been shown to be differentially regulated in malignant tumors, and to play role in carcinogenesis and progression [23].

Hepatocellular expression of claudin-1 was found to be increased in HCV-infected livers [66, 67]. Attenuated expression of claudin-1 closely correlates with the dedifferentiation and portal invasion of hepatocellular carcinoma [35]. Defect in claudin-1 expression increases paracellular permeability in polarized hepatic cell lines, supporting the hypothesis that paracellular bile leakage through deficient TJs is involved in liver pathology observed in NISCH syndrome [28]. In our experiments, the endoderm-like cells at day 8 expressed significantly higher levels of claudin-1 than the hepatocyte-like cells at the end of the differentiation, which is consistent with previous reports demonstrating that claudin-1 is widely expressed in the epithelia [65] .

Claudin-4 expression reported to be a useful marker for distinguishing between biliary tract cancers and hepatocellular carcinomas [7]. The Clostridium perfringens enterotoxin induces cytolysis very rapidly through binding to its receptors [68], which were identified as claudin-4 [23]. Clostridium perfringens enterotoxin binds specifically to hepatocytes, and causes pyogenic liver abscess [68]. Claudin-4

can be found in cholangiocyte tumors and cholangiocytes too [7, 29], and cytokeratin-7 is a conventional markers of cholangiocytes [11, 12]. In our experiments the gene expression of claudin-4 significantly increased and reached the highest level in the cells at the end of the differentiation.

Claudin-5 expression also gradually increased in our experiments of stem cell differentiation. Claudin-5 is usually expressed in endothelial cells [22], but also present in fibrolamellar carcinoma of the liver, in contrast to ordinary hepatocellular carcinoma and cholangiocarcinoma, which lack claudin-5 expression [27, 38]. Our findings that claudin-5 is detected during differentiation from HUES9 is consistent with the observation that certain tumors of epithelial origin deriving from different stages of differentiation express claudin-5 [43]. A significant increase in the expression of claudin-7 was observed in hepatocellular carcinoma (HCC) versus nontumorous tissues [30]. Survival analysis showed a trend toward a better prognosis among patients with overexpression of claudin-7 in tumor tissues [39]. Unlike claudin-1, and 4 expressions, claudin-5, and 7 expressions did not change significantly during the hepatic differentiation of HUES9 cells.

Tricellulin contributes to the structure and function of tricellular contacts of neighboring cells in many epithelial tissues [26, 69]. We found that the tricellulin mRNA expression was slightly elevated in the endoderm-like cells at day 8 of the hepatic differentiation, and subsequently returned to the basal level. Despite the fact that this increase was not significant, immunofluorescence staining revealed normal tricellulin distribution in the differentiated cells at the final stage. It can be speculated that the small, transient elevation in the tricellulin mRNA level during the hepatic differentiation may result in sufficient protein production.

The heparin sulfate proteoglycan agrin selectively deposits in HCC microvessels versus sinusoidal walls, and also accumulates in cholangiocarcinoma [34, 70]. Agrin immunohistochemistry can be used to discriminate between HCCs and benign parenchymal lesions [70, 71]. The gene expression of agrin, which is associated with basement membranes in several tissues, was significantly increased during hepatic differentiation of HUES9 cells. This further suggests the important role of agrin in hepatic proliferation and hepatocarcinogenesis [71].

The matured hepatocytes are highly polarized cells, where intercellular junctions, including TJs, determine cell polarity [32, 65]. Changes in the marker gene, ABC transporter gene and TJ gene expression patterns in our experiments may reflect the *in vivo* hepatocyte differentiation process. Expression patterns of the hepatocyte-specific genes, ABC transporter genes and the TJ genes observed in our study were typical for cells having both hepatocyte and cholangiocyte characteristics [13]. This may be caused by complete polarization of cells, which also observed in hepatocytes during development, leading to adequate targeting of proteins specific to the canalicular membrane [13, 14, 21] . Our study indicates that the main cell types in the heterogeneous cell cultures obtained by the end of the hepatic differentiation of HUES9 cells were almost matured hepatocytes and cholangiocytes.

In conclusion, our findings demonstrate that HUES9 cells can be differentiated into typical liver cells with appropriate morphology, functional properties, and characteristic expression pattern. The hepatocyte-like cells differentiated from HUES9 cells can serve not only as cell source to substitute human hepatocytes, but also provide a model that may reveal molecular mechanisms of the pathogenesis of different types of liver cancers, thus, helping to develop novel therapeutic strategies for primary liver tumors.

Acknowledgments

This work has been supported by grants from the Hungarian Scientific Research Fund (OTKA K108548), Ministry of National Development (KTIA_OTKA_CK80283 and KTIA_AIK_12-1-2012-0025), and the Momentum Program of the Hungarian Academy of Sciences (LP 2012-025).

We appreciate the gift of HUES1 and HUES9 cell lines provided by Dr. Douglas Melton. We thank Andrea Balogh (Department of Immunology, Eötvös Loránd University, Budapest, Hungary) for the critical reading of the manuscript.

References

1. Schulz, T.C., et al., *A scalable system for production of functional pancreatic progenitors from human embryonic stem cells.* PLoS One, 2012. **7**(5): p. e37004.
2. Kirkeby, A., et al., *Generation of regionally specified neural progenitors and functional neurons from human embryonic stem cells under defined conditions.* Cell Rep, 2012. **1**(6): p. 703-14.
3. Nicoleau, C., et al., *Human pluripotent stem cell therapy for Huntington's disease: technical, immunological, and safety challenges human pluripotent stem cell therapy for Huntington's disease: technical, immunological, and safety challenges.* Neurotherapeutics, 2011. **8**(4): p. 562-76.
4. Moon, S.H., et al., *A system for treating ischemic disease using human embryonic stem cell-derived endothelial cells without direct incorporation.* Biomaterials, 2011. **32**(27): p. 6445-55.
5. Murry, C.E. and G. Keller, *Differentiation of embryonic stem cells to clinically relevant populations: lessons from embryonic development.* Cell, 2008. **132**(4): p. 661-80.
6. Vosough, M., et al., *Cell-based therapeutics for liver disorders.* Br Med Bull, 2011. **100**: p. 157-72.
7. Lodi, C., et al., *Claudin-4 differentiates biliary tract cancers from hepatocellular carcinomas.* Mod Pathol, 2006. **19**(3): p. 460-9.
8. Nemeth, Z., et al., *Claudin-1, -2, -3, -4, -7, -8, and -10 protein expression in biliary tract cancers.* J Histochem Cytochem, 2009. **57**(2): p. 113-21.
9. Kinugasa, T., et al., *Increased claudin-1 protein expression in hepatic metastatic lesions of colorectal cancer.* Anticancer Res, 2012. **32**(6): p. 2309-14.
10. Van Eyken, P., et al., *The development of the intrahepatic bile ducts in man: a keratin-immunohistochemical study.* Hepatology, 1988. **8**(6): p. 1586-95.
11. Paku, S., et al., *Immunohistochemical analysis of cytokeratin 7 expression in resting and proliferating biliary structures of rat liver.* Hepatology, 2005. **42**(4): p. 863-70.
12. Vestentoft, P.S., et al., *Three-dimensional reconstructions of intrahepatic bile duct tubulogenesis in human liver.* BMC Dev Biol, 2011. **11**: p. 56.
13. Dezso, K., et al., *Architectural and immunohistochemical characterization of biliary ductules in normal human liver.* Stem Cells Dev, 2009. **18**(10): p. 1417-22.
14. Mayer, R., et al., *Expression of the MRP gene-encoded conjugate export pump in liver and its selective absence from the canalicular membrane in transport-deficient mutant hepatocytes.* J Cell Biol, 1995. **131**(1): p. 137-50.
15. Bodo, A., et al., *Differential modulation of the human liver conjugate transporters MRP2 and MRP3 by bile acids and organic anions.* J Biol Chem, 2003. **278**(26): p. 23529-37.
16. Fitz, J.G., et al., *Regulation of membrane chloride currents in rat bile duct epithelial cells.* J Clin Invest, 1993. **91**(1): p. 319-28.
17. Guo, Y., M. Lubbert, and M. Engelhardt, *CD34- hematopoietic stem cells: current concepts and controversies.* Stem Cells, 2003. **21**(1): p. 15-20.

18. Apati, A., et al., *High level functional expression of the ABCG2 multidrug transporter in undifferentiated human embryonic stem cells.* Biochim Biophys Acta, 2008. **1778**(12): p. 2700-9.
19. Sarkadi, B., et al., *Evaluation of ABCG2 expression in human embryonic stem cells: crossing the same river twice?* Stem Cells, 2010. **28**(1): p. 174-6.
20. Padmanabhan, R., et al., *Regulation and expression of the ATP-binding cassette transporter ABCG2 in human embryonic stem cells.* Stem Cells, 2012. **30**(10): p. 2175-87.
21. Furuse, M., H. Sasaki, and S. Tsukita, *Manner of interaction of heterogeneous claudin species within and between tight junction strands.* J Cell Biol, 1999. **147**(4): p. 891-903.
22. Amasheh, S., et al., *Contribution of claudin-5 to barrier properties in tight junctions of epithelial cells.* Cell Tissue Res, 2005. **321**(1): p. 89-96.
23. Hewitt, K.J., R. Agarwal, and P.J. Morin, *The claudin gene family: expression in normal and neoplastic tissues.* BMC Cancer, 2006. **6**: p. 186.
24. Mineta, K., et al., *Predicted expansion of the claudin multigene family.* FEBS Lett, 2011. **585**(4): p. 606-12.
25. Furuse, M., et al., *Claudin-1 and -2: novel integral membrane proteins localizing at tight junctions with no sequence similarity to occludin.* J Cell Biol, 1998. **141**(7): p. 1539-50.
26. Riazuddin, S., et al., *Tricellulin is a tight-junction protein necessary for hearing.* Am J Hum Genet, 2006. **79**(6): p. 1040-51.
27. Patonai, A., et al., *Claudins and tricellulin in fibrolamellar hepatocellular carcinoma.* Virchows Arch, 2011. **458**(6): p. 679-88.
28. Grosse, B., et al., *Claudin-1 involved in neonatal ichthyosis sclerosing cholangitis syndrome regulates hepatic paracellular permeability.* Hepatology, 2012. **55**(4): p. 1249-59.
29. Bunthot, S., et al., *Overexpression of claudin-4 in cholangiocarcinoma tissues and its possible role in tumor metastasis.* Asian Pac J Cancer Prev, 2012. **13 Suppl**: p. 71-6.
30. Jakab, C., et al., *Claudin-7 protein differentiates canine cholangiocarcinoma from hepatocellular carcinoma.* Histol Histopathol, 2010. **25**(7): p. 857-64.
31. Schulzke, J.D. and M. Fromm, *Tight junctions: molecular structure meets function.* Ann N Y Acad Sci, 2009. **1165**: p. 1-6.
32. Forster, C., *Tight junctions and the modulation of barrier function in disease.* Histochem Cell Biol, 2008. **130**(1): p. 55-70.
33. Tatrai, P., et al., *Agrin, a novel basement membrane component in human and rat liver, accumulates in cirrhosis and hepatocellular carcinoma.* Lab Invest, 2006. **86**(11): p. 1149-60.
34. Batmunkh, E., et al., *Comparison of the expression of agrin, a basement membrane heparan sulfate proteoglycan, in cholangiocarcinoma and hepatocellular carcinoma.* Hum Pathol, 2007. **38**(10): p. 1508-15.
35. Higashi, Y., et al., *Loss of claudin-1 expression correlates with malignancy of hepatocellular carcinoma.* J Surg Res, 2007. **139**(1): p. 68-76.
36. Sobel, G., et al., *Increased expression of claudins in cervical squamous intraepithelial neoplasia and invasive carcinoma.* Hum Pathol, 2005. **36**(2): p. 162-9.

37. Jakab, C., et al., *Expression of claudin-1, -3, -4, -5 and -7 proteins in low grade colorectal carcinoma of canines.* Histol Histopathol, 2010. **25**(1): p. 55-62.
38. Miettinen, M., M. Sarlomo-Rikala, and Z.F. Wang, *Claudin-5 as an immunohistochemical marker for angiosarcoma and hemangioendotheliomas.* Am J Surg Pathol, 2011. **35**(12): p. 1848-56.
39. Brokalaki, E.I., et al., *Claudin-7 expression in hepatocellular carcinoma.* Transplant Proc, 2012. **44**(9): p. 2737-40.
40. Ersoz, S., et al., *Prognostic importance of Claudin-1 and Claudin-4 expression in colon carcinomas.* Pathol Res Pract, 2011. **207**(5): p. 285-9.
41. Tsutsumi, K., et al., *Claudin-4 expression predicts survival in pancreatic ductal adenocarcinoma.* Ann Surg Oncol, 2012. **19 Suppl 3**: p. S491-9.
42. Agarwal, R., T. D'Souza, and P.J. Morin, *Claudin-3 and claudin-4 expression in ovarian epithelial cells enhances invasion and is associated with increased matrix metalloproteinase-2 activity.* Cancer Res, 2005. **65**(16): p. 7378-85.
43. Lappi-Blanco, E., et al., *Divergence of tight and adherens junction factors in alveolar epithelium in pulmonary fibrosis.* Hum Pathol, 2013. **44**(5): p. 895-907.
44. Resnick, M.B., et al., *Claudin-1 is a strong prognostic indicator in stage II colonic cancer: a tissue microarray study.* Mod Pathol, 2005. **18**(4): p. 511-8.
45. Kominsky, S.L., *Claudins: emerging targets for cancer therapy.* Expert Rev Mol Med, 2006. **8**(18): p. 1-11.
46. Dezso, K., et al., *Structural analysis of oval-cell-mediated liver regeneration in rats.* Hepatology, 2012. **56**(4): p. 1457-67.
47. Mateizel, I., et al., *Establishment of hESC lines from the inner cell mass of blastocyst-stage embryos and single blastomeres of 4-cell stage embryos.* Methods Mol Biol, 2012. **873**: p. 81-112.
48. Xu, C., et al., *Feeder-free growth of undifferentiated human embryonic stem cells.* Nat Biotechnol, 2001. **19**(10): p. 971-4.
49. Chen, Y., et al., *Instant hepatic differentiation of human embryonic stem cells using activin A and a deleted variant of HGF.* Cell Transplant, 2006. **15**(10): p. 865-71.
50. Cai, J., et al., *Directed differentiation of human embryonic stem cells into functional hepatic cells.* Hepatology, 2007. **45**(5): p. 1229-39.
51. Baharvand, H., et al., *Differentiation of human embryonic stem cells into hepatocytes in 2D and 3D culture systems in vitro.* Int J Dev Biol, 2006. **50**(7): p. 645-52.
52. Vosough, M., et al., *Generation of functional hepatocyte-like cells from human pluripotent stem cells in a scalable suspension culture.* Stem Cells Dev, 2013. **22**(20): p. 2693-705.
53. Rambhatla, L., et al., *Generation of hepatocyte-like cells from human embryonic stem cells.* Cell Transplant, 2003. **12**(1): p. 1-11.
54. Turksen, K., *Claudins and cancer stem cells.* Stem Cell Rev, 2011. **7**(4): p. 797-8.
55. Sell, S. and H.L. Leffert, *Liver cancer stem cells.* J Clin Oncol, 2008. **26**(17): p. 2800-5.
56. Halasz, J., et al., *Claudin-1 and claudin-2 differentiate fetal and embryonal components in human hepatoblastoma.* Hum Pathol, 2006. **37**(5): p. 555-61.

57. Adewumi, O., et al., *Characterization of human embryonic stem cell lines by the International Stem Cell Initiative.* Nat Biotechnol, 2007. **25**(7): p. 803-16.
58. Erdei, Z., et al., *Dynamic ABCG2 expression in human embryonic stem cells provides the basis for stress response.* Eur Biophys J, 2013. **42**(2-3): p. 169-79.
59. Papp, V., et al., *Expansion of Hepatic Stem Cell Compartment Boosts Liver Regeneration.* Stem Cells Dev, 2013.
60. Basma, H., et al., *Differentiation and transplantation of human embryonic stem cell-derived hepatocytes.* Gastroenterology, 2009. **136**(3): p. 990-9.
61. Thomson, J.A., et al., *Embryonic stem cell lines derived from human blastocysts.* Science, 1998. **282**(5391): p. 1145-7.
62. Silva, J. and A. Smith, *Capturing pluripotency.* Cell, 2008. **132**(4): p. 532-6.
63. Osafune, K., et al., *Marked differences in differentiation propensity among human embryonic stem cell lines.* Nat Biotechnol, 2008. **26**(3): p. 313-5.
64. Turanyi, E., et al., *Immunohistochemical classification of ductular reactions in human liver.* Histopathology, 2010. **57**(4): p. 607-14.
65. Tsukita, S., et al., *Tight junction-based epithelial microenvironment and cell proliferation.* Oncogene, 2008. **27**(55): p. 6930-8.
66. Zadori, G., et al., *Examination of claudin-1 expression in patients undergoing liver transplantation owing to hepatitis C virus cirrhosis.* Transplant Proc, 2011. **43**(4): p. 1267-71.
67. Farquhar, M.J., et al., *Hepatitis C virus induces CD81 and claudin-1 endocytosis.* J Virol, 2012. **86**(8): p. 4305-16.
68. Jarmund, T. and W. Telle, *Binding of Clostridium perfringens enterotoxin to hepatocytes, small intestinal epithelial cells and Vero cells.* Acta Pathol Microbiol Immunol Scand B, 1982. **90**(5): p. 377-81.
69. Korompay, A., et al., *Tricellulin expression in normal and neoplastic human pancreas.* Histopathology, 2012. **60**(6B): p. E76-86.
70. Tatrai, P., et al., *Agrin and CD34 immunohistochemistry for the discrimination of benign versus malignant hepatocellular lesions.* Am J Surg Pathol, 2009. **33**(6): p. 874-85.
71. Somoracz, A., et al., *Agrin immunohistochemistry facilitates the determination of primary versus metastatic origin of liver carcinomas.* Hum Pathol, 2010. **41**(9): p. 1310-9.

Figures legends

Fig. 1 Hepatic differentiation of HUES cells

(a) Schematic illustration of the 3-stage differentiation procedure. Human embryonic stem cells were maintained undifferentiated in MEF conditioned medium for 3 days (Stage 1), then were cultured in the presence of activin A (50 ng/ml) for 5 days (Stage 2), finally, endodermal-like cells were cultured in the presence of HGF (20 ng/ml) without activin A for 7 days in Matrigel-coated culture dishes (Stage 3).

(b-d) Morphology of HUES9 cells and their derivatives during differentiation. Representative images of undifferentiated HUES9 at day 3 (b) endoderm-like cells at day 8 (c), and hepatocyte-like cells at day 15 (d) are displayed. Scale bar = 50 μm. For better perceptibility a DIC image with higher magnification at the final stage is also shown (e). Scale bar = 10 μm. By the end of differentiation the cells exhibited polygonal shape and were enriched in cytoplasmic granules, which morphology is characteristic of human hepatocytes in culture.

Fig. 2 Assessment of hepatocyte functions in cells differentiated from HUES9 cells

Periodic Acid Schiff-staining (a-d) demonstrates the glycogen production and storage in HUES9 cell-derived cells (b) and primary hepatocytes (d). In contrast, no PAS staining was observed in undifferentiated HUES9 cells (a) or MDCK cells (c), which served as a negative control. Scale bar = 20 μm.

ICG uptake (e, f, g, h). (e-h) Indocyanin Green uptake and release assay evaluates the capability of cells for accumulation and extrusion of the organic anion dye. HUES9-derived differentiated cells at day 15 accumulated ICG (e), whereas no dye uptake was observed in undifferentiated HUES9 cells (g). The ICG was released from the differentiated cells 6 hours after dye uptake (f). Representative images from three independent experiments are displayed. Scale bar = 50 μm.

Fig. 3 mRNA expression levels of differentiation markers during the course of hepatic differentiation of HUES9 cells

Gene expressions of various stem cell markers, liver markers, and cytokeratins were measured by RT-PCR at different stages of differentiation as indicated.

(a) Expression levels of the stem cell markers, Oct3/4 and Nanog significantly decreased, whereas the hepatic markers, α-fetoprotein (AFP) and albumin (ALB) were significantly induced during hepatic differentiation of HUES9 cells. (b) The expression level of Cytokeratin-7 increased significantly, while Cytokeratin-19 was hardly induced. No change in the expression levels of Cyokeratin-8 and Cytokeratin-18 was observed in the course of differentiation. Data are shown as mean±SD of three independent experiments. Asterisks denote significant changes ($p<0.05$).

Fig. 4 Hepatic ABC-transporter genes expression levels during hepatic differentiation of HUES9 cells

The substantial expression level of ABCG2 found in undifferentiated HUES9 cells gradually decreased until the end of the endodermal stage, and then robustly rose by the end of the differentiation exceeding the expression level observed at the pluripotent stage. The mRNA level of the organic anion transporter, ABCC2 (MRP2) significantly increased during hepatic differentiation of HUES9 cells. Similarly, the expression of ABCC7 (CFTR), which is characteristic of cholangiocytes, was also significantly induced Data are shown as mean±SD of three independent experiments. Asterisks denote significant changes ($p<0.05$).

Fig. 5 Changes in gene expression levels of tight junction and extracellular matrix components typical of liver cells

The mRNA expressions of claudin-1 and claudin-4 were significantly increased, while that of claudin-5 exhibited only small changes during hepatic differentiation of HUES9 cells. No change in claudin-7 expression was observed. The gene expression of agrin was significantly increased, whereas tricellulin expression level did not change. Data are shown as mean±SD of three independent experiments. Asterisks denote significant changes ($p<0.05$).

Fig. 6 Expression and subcellular localization of tight junction proteins in HUES9-derived hepatic cells

HUES9 cells were differentiated toward the hepatic lineage, and immunostained for claudin-1, -4, -5, -7, and tricellulin proteins. Representative confocal microscopy images of cultures at the final stage of differentiation are shown. For the control experiment, the primary antibody was omitted from the staining procedure. The studied TJ components are expressed in the differentiated cells, and predominantly localized to the plasma membrane. In addition, intracellular expression of claudin-4 and -7 is also observed. Scale bar = 10 μm.

table
Click here to download table: Table1.doc

Table 1. Primers used in RT-PCR analyses

Gene Name	Primer sequence (5'- 3')		Product length (bp)	Annealing temperature (°C)	Gene bank code
	Sense	Antisense			
ABL	ACGAGTCTGGTTGATGCTGTG	GGCGGACTGTGGCTTTGG	105	61	NM_007313
Oct3/4	TGGGCTCGAGAAGGATGTG	GCATAGTCGCTGCTTGATCG	78	61	NM_002701
Nanog	TGAACCTCAGCTACAAACAG	AACTGCATGCAGGACTGCA	350	61	NM_024865
Alpha-fetoprotein (AFP)	TGCAGCCAAAGTGAAGAGGGAAGA	CATAGCGAGCAGCCCAAAGAAGAA	217	61	NM_001134
Albumin (ALB)	TGAGAAAACGCCAGTAAGTGAC	TGCGAAATCATCCATAACAGC	265	61	NM_000477
ABCG2	TACCTGTATAGTGTACTTCAT	GGTCATGAGAAGTGTTGCTA	159	61	NM_004827
ABCC2 (MRP2)	TCCTTGCGCAGCTGGATTACAT	TCGCTGAAGTGAGAGTAGATTG	202	61	NM_000392
ABCC7 (CFTR)	CATTTTTGGCCTTCATCACATT	TGCCTTCCGAGTCAGTTTCAG	474	61	NM_000492
Cytokeratin-7 (CK-7)	CAGTGGCGGTGGCATTGG	CGGATGGAATAAGCCTTCAGGAG	105	61	NM_005556
Cytokeratin-8 (CK-8)	CTCCTCACCAAGAAGCAG	CCTGATGGACATGGTAGAG	94	61	NM_002273
Cytokeratin-18 (CK-18)	GAGATCGAGGCTCTCAAGGA	CAAGCTGGCCTTCAGATTTC	357	61	NM_000224
Cytokeratin-19 (CK-19)	TGACACCATTCCTCCCTTCCC	AGCACGGACGGAGCAACC	119	61	NM_002276
Claudin-1	GTGCGATATTTCTTCTTGCAGGTC	TTCGTACCTGGCATTGACTGG	113	61	NM_021101
Claudin-4	GGCTGCTTTGCTGCAACTGTC	GAGCCGTGGCACCTTACACG	108	61	NM_001305
Claudin-5	TTCCTGAAGTGGTGTCACCTGAAC	TGGCAGCTCTCAATCTTCACAG	97	61	NM_003277
Claudin-7	CATCGTGGCAGGTCTTGCC	GATGGCAGGGCCAAACTCATAC	118	61	NM_001307
Agrin	TCGAGTACCTCAACGCTGTGACC	CCAGTGCCACATAGTCTGCCC	198	61	NM_198576
Tricellulin	TGGAACAACAGGAGATAAATGAGC	GTCTCTTTGTCTGTCACCACTG	86	61	NM_144724

Figure 3

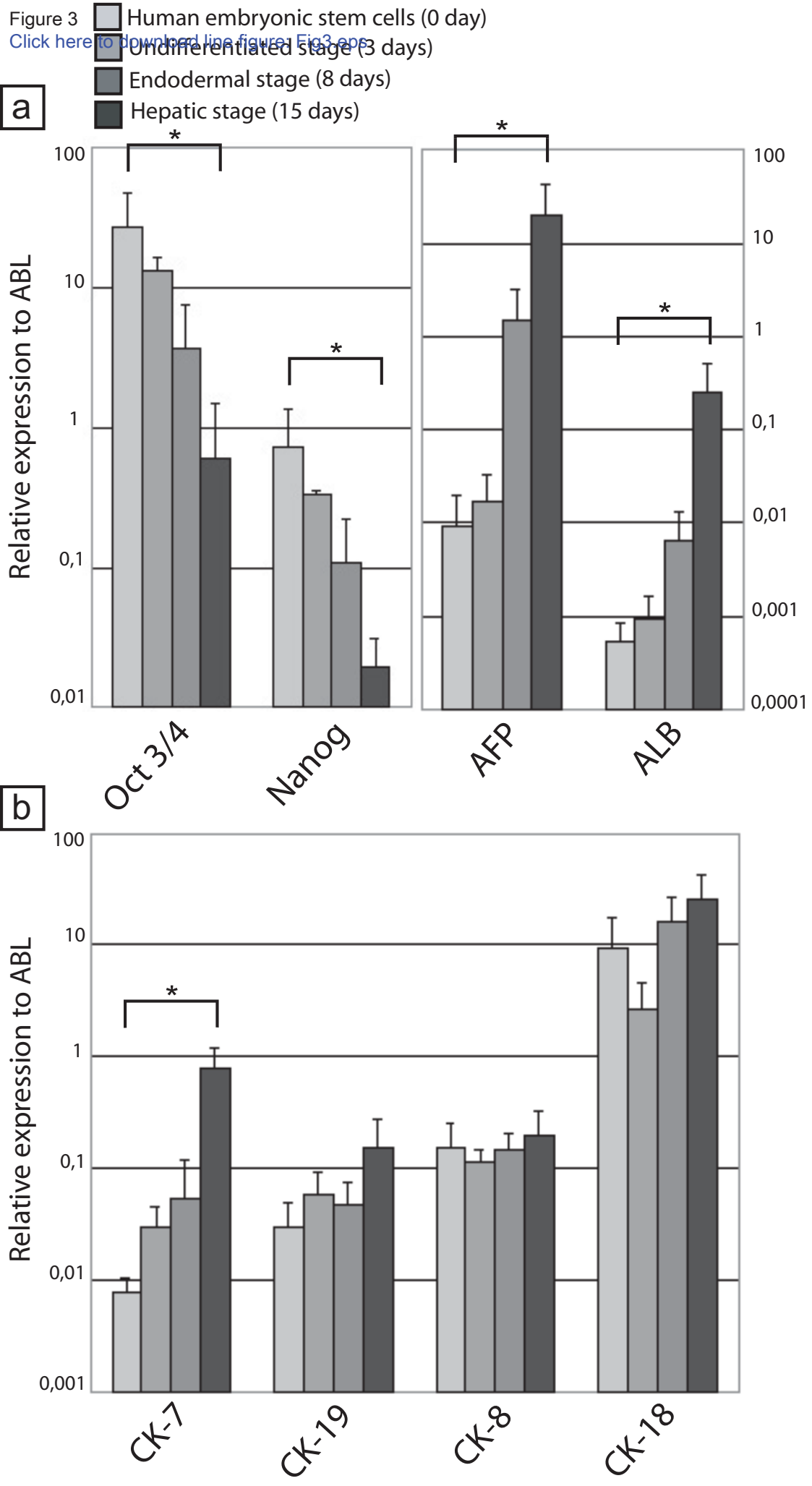

Figure 4
Click here to download line figure: Fig4.eps

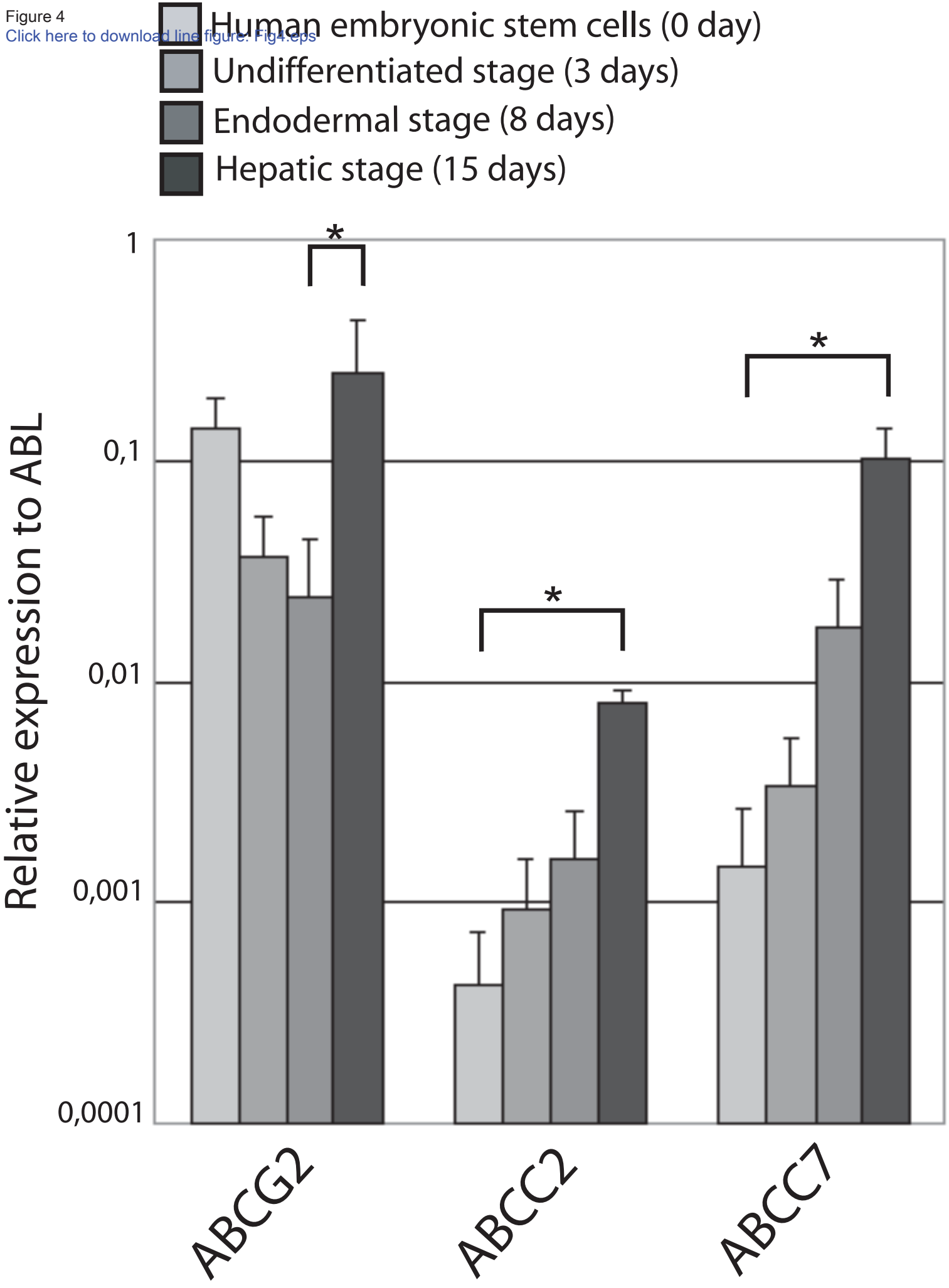

Figure 5
Click here to download line figure: Fig5.eps

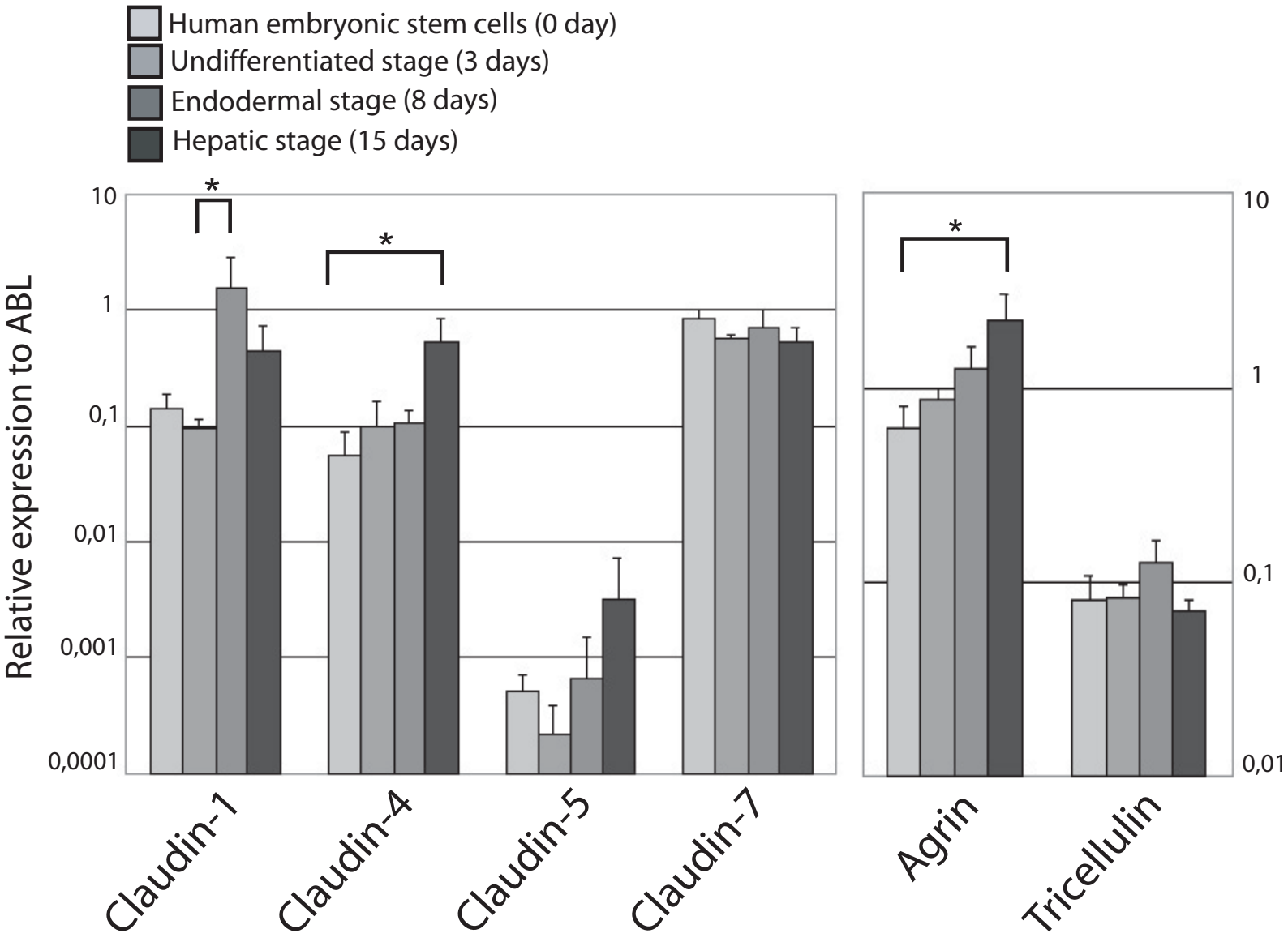

Figure 1 (greyscale)
Click here to download high resolution image

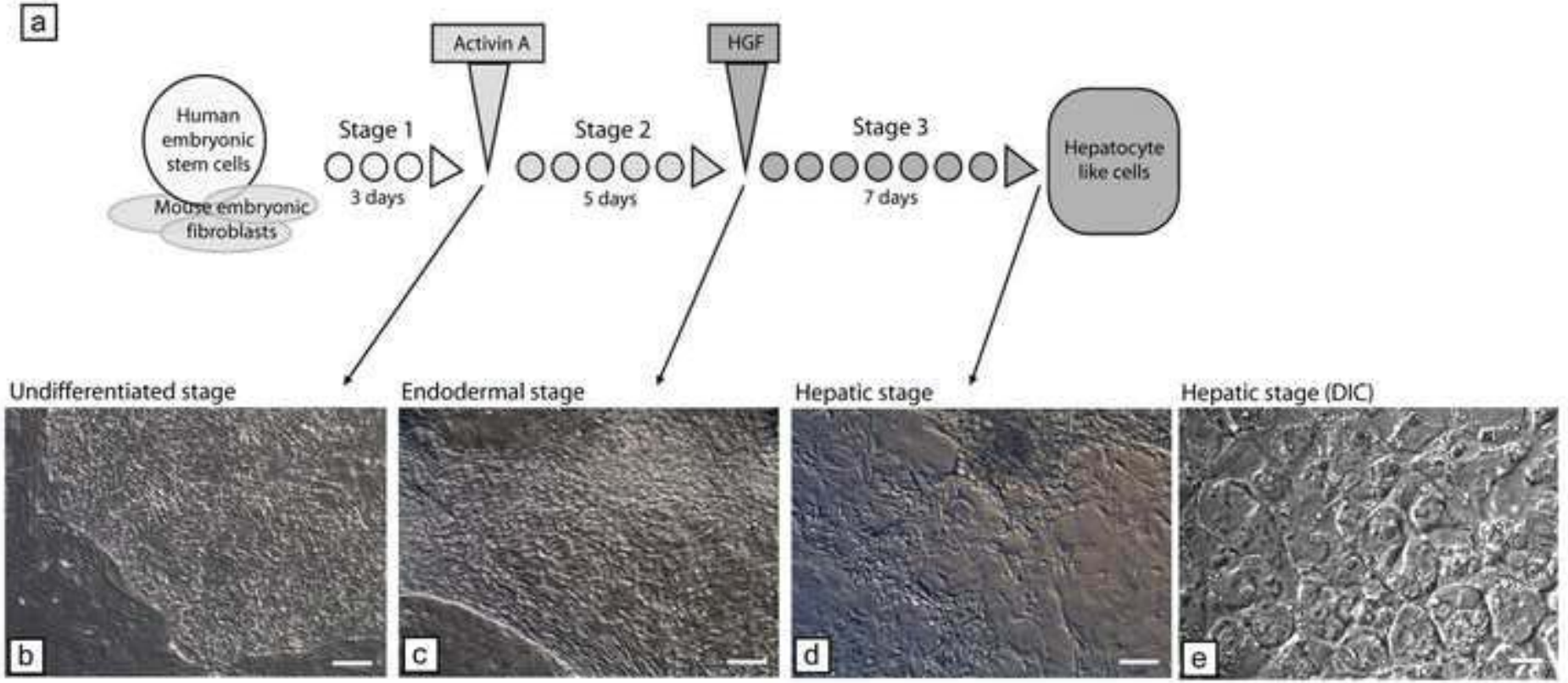

Figure 2
Click here to download high resolution image

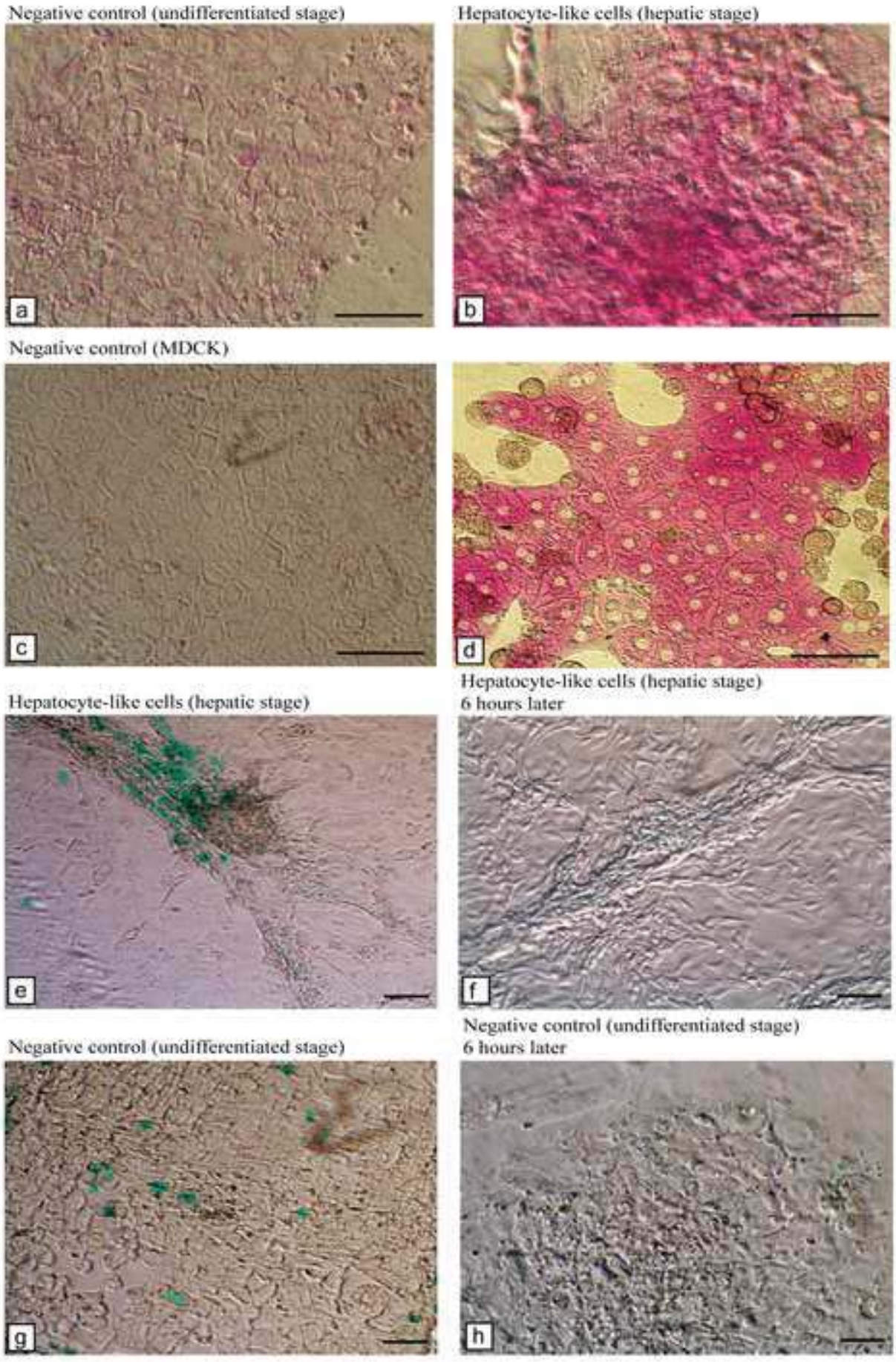

Figure 6
Click here to download high resolution image